JOURNAL OF BACTERIOLOGY, Mar. 2007, p. 1783–1793 Vol. 189, No. 5
0021-9193/07/$08.00+0 doi:10.1128/JB.01230-06

Signal Recognition Particle-Dependent Inner Membrane Targeting of the PulG Pseudopilin Component of a Type II Secretion System▽

Olivera Francetic,[1] Nienke Buddelmeijer,[1] Shawn Lewenza,[1]
Carol A. Kumamoto,[2] and Anthony P. Pugsley[1]*

Molecular Genetics Unit and CNRS URA2172, Institut Pasteur, Paris 75724, France,[1] and Department of Molecular Biology and Microbiology, Tufts University School of Medicine, Boston, Massachusetts 02111[2]

Received 5 August 2006/Accepted 1 December 2006

The pseudopilin PulG is an essential component of the pullulanase-specific type II secretion system from *Klebsiella oxytoca*. PulG is the major subunit of a short, thin-filament pseudopilus, which presumably elongates and retracts in the periplasm, acting as a dynamic piston to promote pullulanase secretion. It has a signal sequence-like N-terminal segment that, according to studies with green and red fluorescent protein chimeras, anchors unassembled PulG in the inner membrane. We analyzed the early steps of PulG inner membrane targeting and insertion in *Escherichia coli* derivatives defective in different protein targeting and export factors. The β-galactosidase activity in strains producing a PulG-LacZ hybrid protein increased substantially when the *dsbA*, *dsbB*, or all *sec* genes tested except *secB* were compromised by mutations. To facilitate analysis of native PulG membrane insertion, a leader peptidase cleavage site was engineered downstream from the N-terminal transmembrane segment (PrePulG*). Unprocessed PrePulG* was detected in strains carrying mutations in *secA*, *secY*, *secE*, and *secD* genes, including some novel alleles of *secY* and *secD*. Furthermore, depletion of the Ffh component of the signal recognition particle (SRP) completely abolished PrePulG* processing, without affecting the Sec-dependent export of periplasmic MalE and RbsB proteins. Thus, PulG is cotranslationally targeted to the inner membrane Sec translocase by SRP.

The pullulanase type II secretion system (T2SS) of *Klebsiella oxytoca*, the Pul secreton, is a prototype of a family of membrane protein complexes dedicated to the transport of folded proteins from the periplasm to the extracellular milieu (49). T2SS machineries share a common origin and architecture and functional properties with systems involved in type IV pilus assembly and retraction, DNA uptake, and natural competence (64). Central to these machineries is their ability to assemble and disassemble filaments that either remain periplasmic and function in protein secretion (pseudopili) or extend well beyond the cell surface and play a role in adhesion, surface motility, or microcolony or biofilm formation (type IV pili) (12). The pseudopili and the closely related class A type IV pili are composed of one major pilin subunit and several minor pilins. Type IVA pilins and T2SS pseudopilins have highly conserved N-terminal regions with properties reminiscent of signal sequences except for their cleavage and N methylation on the N-terminal, cytoplasmic side of the hydrophobic region by a specific prepilin signal peptidase/*N*-methylase (40). This N-terminal hydrophobic helix leads directly into a 30-residue-long amphipathic α-helical region that is less well conserved and is followed by a globular domain composed of four antiparallel beta-sheets (24). In addition, type IVA pilins have a highly variable loop between 2 disulfide-bonded cysteine residues at their C-terminal ends (12).

The predicted topology of PrePulG in the inner membrane (IM) is that of a type II bitopic membrane protein, with an N-in, C-out orientation. Removal of the positively charged N-terminal region by prepilin peptidase renders PulG competent for assembly. Two assembly factors common to the T2SS and type IV pilus assembly and retraction system, a polytopic IM protein of the PilC family (PulF in the Pul secreton) and an oligomeric ATPase of the PilB (VirB11) family (PulE) (36), probably catalyze filament polymerization. Nevertheless, their direct role remains to be demonstrated in an in vitro system and they could also be involved in pseudopilin precursor export from the cytoplasm.

PulG, the major pseudopilin of the Pul secreton, is assembled into a pilus structure on the cell surface when overproduced (50). Sheering and purification of these pili revealed PulG as their unique component (24), suggesting that minor pilins remain cell envelope associated at the filament base. The crystal structure of residues 25 to 146 of PulG revealed the same basic architecture as that of type IV pilins of *Pseudomonas aeruginosa* or *Neisseria gonorrhoeae* (24). Docking of the PulG structure onto the PulG filament, visualized by electron microscopy, enabled a model to be proposed in which the filament is a one-start, left-handed helix with 17 monomers and four helical turns per repeat unit (24).

Despite the wealth of structural data on type IV pili/pseudopili and their subunits, very little is known about the early events involved in pseudopilus biogenesis. Here we analyze the targeting and insertion of the newly synthesized pilin subunits into the IM of *Escherichia coli* by using a combination of in vivo gene fusion and biochemical approaches. The subcellular location of pilin subunits in the absence or presence of the other Pul secreton factors was analyzed in vivo using PulG fused to green and red fluorescent proteins. Given the high level of structural conservation among pseudopilins and type IV pilins,

* Corresponding author. Mailing address: Molecular Genetics Unit, Institut Pasteur, 25 Rue du Dr. Roux, 75724 Paris Cedex 15, France. Phone: 33-145688494. Fax: 33-1456788960. E-mail: max@pasteur.fr.
▽ Published ahead of print on 8 December 2006.

TABLE 1. *Escherichia coli* strains used in this study

Strain	Genotype	Source or reference
MC4100	(F$^-$) Δ*lac-169 araD139 thiA rpsL relA motA rbsR*	Laboratory collection
MM52	MC4100 *secA51*(Ts)	35
MM18	MC4100 λ*malE-lacZ*72-47	22
TY22	MC4100 *rpsE ompT*::*kan zdh*::Tn*10 secY40*	4, 33, 57
AD208	MC4100 *ompT*::*kan zdh*::Tn*10 secY39*	4, 33, 57
JCB656	MC4100 λ*malF-lacZ102 dsbA*::*kan malT*(Con)	J. Bardwell
MC4100Δ*secB*	MC4100 Δ*secB*	P. Delepelaire
CK1637	*araD* Δ*(lac-pro)XIII* Rif^r Nal^r *argE*(Am) *mtl-2 recA1*(Sm^s) F′ *lacI*^{q1}	C. Kumamoto
WAM121	MC4100 *ara*$^+$ *ffh*::*kan attB*::ori R6K p*araBAD*::*ffh tet*	14, H. Bernstein
PAP7460	MC4100 Δ*malE444* pAPIP501 (F′ *lacI*^{q1} Δ*lacZM15 proAB*$^+$ Tn*10*)	Laboratory collection
JCB571	MC1000 *phoR zih-12*::Tn*10 dsbA*::*kan-1*	6
IQ85	MC4100 *secY24*(Ts) *zhd-33*::Tn*10*	K. Ito
PS266	MC4100 *secE15*(Cs)	51
OFM1004	MC4100 *secY108*	This study
PAP5237	MC4100 *dsbA*::*kan*	This study
PAP5250	MC4100 *dsbB*::*kan*	This study
OF670	OFM1004 *zjb*::Tn*5 malE18-1*	This study
OFM4004	MC4100 *secD4004*(Cs)	This study
OFM1610	MC4100 *secE1610*	This study
OFM7004	MC4100 *secA7004*	This study
PAP9102	MC4100 Δ(*att*λ-*lom)*::*bla lacI*^{q1} *gfp-pulG*	This study
PAP9121	MC4100 Δ(*att*λ-*lom)*::*bla lacI*^{q1} *gfp*	This study
PAP7500	MC4100::*pulS pulAB pulCO* (F′ *lacI*^{q1} Δ*lacZM15 proAB*$^+$ Tn*10*)	Laboratory collection
PAP7500BG	PAP7500 *pulB*::*km* Δ*pulG*	Laboratory collection

TABLE 2. Oligonucleotides used in this study

Oligonucleotide	Nucleotide sequence (5′–3′)
PulGBamHI	GTAGGATCCTTCCCGATCGTCCAGTTG
PulG-BglII	CCGAGATCTGTGATTGTTCTAATGGAG
PulGEco5′	CGGAATTCGAGTATGTGATTGTTCTAATGGAG
PulGNco3′	GACCATGGCCATCGCCGGCACCACGAGGCTG
SecEL	CCGAATTCCGAAAAGCTAATACGCGTTTC
SecER	CAAGGATCCGAAAACGCCTGAACGACGTAC
SecDL	CACAAGCTTCGAAAGGCACCATGAAGG
SecDR	CCACTCGAGGTTCAACAGTATATTCCTGTG
SecDseq	CGTGCGAAAGAGATTCTGGGTGCGAC
SecD2	GCATCCCGTATACCACTGTTCGTAAAG
SecFL	CAAGAATTCGCGCGTCAAGAAGCTGTC
SecFR	CAAGGATCCGGATTTTCGCAATCTCC
Ngfp-pulG-5	CGAGAATTCAACAACAACCAACGACAGCGCGGATTC
Ngfp-pulG-3	CCGTCGAAGCTTCTATTTCTTCCCGATCGTCCAG
XbaI-RFP-5	CTAGTCTAGAATGGCCTCCTCCGAGGACGTCATCAAGG
HindIIIRFP-3	CCTGAAGCTTTTAGGCGCCGGTGGAGTGGCGG
PulGERI-5	CGAGAATTCATGCAACGACAGCGCGGATTC
GrfpXbaI-3	CTAGTCTAGATTTCTTCCCGATCGTCCAG

the conclusions drawn from this study probably apply to this entire protein family.

MATERIALS AND METHODS

Bacterial strains, growth conditions, and genetic techniques. *E. coli* strains used in this study are listed in Table 1. Luria-Bertani (LB) broth and agar, tetrazolium-lactose agar, MacConkey maltose agar, or minimal M63 medium was prepared as described previously (32). When appropriate, media were supplemented with maltose (0.4%), lactose (0.4%), arabinose (0.2%), glycerol (0.5%), or glucose (0.2%). Temperature-sensitive phenotypes were tested at 20°C (cold sensitive) or 42°C (heat sensitive) on LB agar. For β-galactosidase and fractionation assays, temperature-sensitive strains were grown under semipermissive conditions (30°C for cold-sensitive and 37°C for heat-sensitive strains), unless otherwise indicated. Antibiotics were used at the following concentrations: tetracycline, 10 μg/ml; chloramphenicol, 25 μg/ml; ampicillin (Amp), 100 μg/ml; kanamycin, 50 μg/ml; spectinomycin, 100 μg/ml, and streptomycin, 100 μg/ml. Generalized transduction with P1*vir* phage and bacterial conjugation were performed as described previously (32).

Plasmid construction and molecular biology techniques. DNA manipulations, plasmid purification, and DNA transformation were performed essentially as described previously (47). PCR amplification was performed using *Pfu* (Invitrogen) or Phusion (Finnzymes) DNA polymerase in buffers supplied by the manufacturers. Oligonucleotide primers used for PCR and DNA sequence analysis are listed in Table 2. Plasmid pCHAP8075 containing the *pulG-lacZ* fusion was constructed by cloning the *pulG* gene, PCR amplified without the stop codon by using primers PulGBamHI and PulGBglII, into the BamHI site of pOF13 (17). Plasmid pCHAP8086 was made by cloning the DNA fragment encoding the prepilin signal sequence of PulG, PCR amplified using primers PulGEco5′ and PulGNco3′, into the EcoRI and NcoI sites of pCHAP7010 (*pelB*$_{SP}$-*pulG*$_{25\text{-}140}$His$_6$) (24). This event replaced the PelB signal peptide with the PulG prepilin signal sequence, followed by a leader peptidase cleavage site. The EcoRI-HindIII fragment containing the *pulG*$_{SP}$-*pulG* gene was subcloned into a low-copy-number vector, pHSG575 (56), digested with the same enzymes, giving pCHAP8100. Plasmid pCHAP8095 contained a wild-type *secE* gene, cloned as a PCR fragment generated using primers SecEL and SecER into the EcoRI and BamHI sites of pSU18 (7). Plasmid pCHAP8096 contained a wild-type *secD* gene, PCR amplified using flanking primers SecDL and SecDR, digested with Xho and HindIII, and cloned into the SalI and HindIII sites of pSU19. The wild-type *secF* gene was cloned into the EcoRI and BamHI sites of plasmid pSU19 after PCR amplification using primers SecFL and SecFR, giving plasmid pCHAP8092.

Plasmid pCHAP7506 (encoding green fluorescent protein [GFP]-PrePulG) was made by cloning the *pulG* gene, PCR amplified using oligonucleotides Ngfp-PulG-5 and Ngfp-pulG-3. The PCR product was inserted into the EcoRI and HindIII sites of vector pDSW204 (63). Integration of the *pulG-gfp* fusion into the *att*λ site of the chromosome of strain MC4100 via λInCh was performed as described previously (9), resulting in strain PAP9102. pCHAP7506 was able to fully restore pullulanase secretion in a strain lacking *pulG*, indicating that processing of GFP-PrePulG by PulO prepilin peptidase produces functional PulG. The monomeric red fluorescent protein (mRFP1) fusion vector pCHAP7520 was made by inserting the mRFP1-encoding gene from plasmid pRSetBmRFP1 (11), PCR amplified using oligonucleotide primers XbaI-RFP-5 and HindIIIRFP-3, into pDSW204. The *pulG* gene, amplified using primers PulGERI-5 and GrfpXbaI-3, was inserted into the EcoRI and XbaI sites of this vector to give pCHAP7516. This plasmid restored to only 20% of wild type the level of pullulanase secretion in a strain lacking *pulG*, presumably because the RFP domain interferes with PulG assembly and functional PulG is not released from PulG-mRFP by proteolysis (39). All plasmid constructs were verified by DNA sequencing. Other plasmids were pCHAP231, carrying all of the *pul* secreton genes

including *pulA* (14), and pCHAP710, carrying all of the *pul* secreton genes except *pulA* (25).

Mutagenesis and selection of Lac$^+$ mutants. *E. coli* Lac$^+$ mutants expressing the *rbsB-lacZ* gene fusion were isolated as follows. *E. coli* strain MC4100 was grown to mid-exponential phase and incubated in the presence of 50 μg/ml of *N*,*N*-nitrosoguanidine for 15 min at 37°C. Bacteria were washed twice in M63 salts solution, resuspended in LB medium, and divided into 16 pools, which were grown out overnight at 30°C. The approximate killing rate was 33%. Mutagenized bacteria were transformed with plasmid pOF21 carrying an *rbsB-lacZ* gene fusion (17), plated on lactose-tetrazolium plates containing ampicillin, and incubated for 48 h at 30°C. Bacteria in pink colonies growing on a white lawn were purified twice on lactose-tetrazolium Amp plates and cured of pOF21 on LB plates containing 5-bromo-4-chloro-3-indolyl-β-D-galactopyranoside (X-Gal). White, Amp-sensitive bacteria were purified twice on the same medium and then retransformed with pOF21 to check that the lesions causing the Lac$^+$ phenotype were linked to the chromosome. Out of a total of 144 mutants tested in this way, 54 contained chromosomal lesions, suggesting that other, plasmid-linked mutations arose spontaneously during growth on selective plates.

Mutant characterization. In addition to nine mutations in the *dsbA* gene, two in *mutT*, and a number of uncharacterized mutations, the RbsB-LacZ Lac$^+$ screen yielded multiple mutations in known *sec* loci (*secA*, *secDF*, *secE*, and *secY*) (O. Francetic and C. Kumamoto, unpublished results). Pulse-chase analysis showed that these mutations conferred export defects of both MalE and RbsB. Four of these mutations were characterized in the present study. The mutation conferring the Lac$^+$ phenotype in strain OLFM1004 was 90% cotransduced with the Sm^r marker *rpsL* at min 72, indicating that the lesion is linked tightly to the *secY* locus. To facilitate its genetic analysis, this mutation was combined with a mutation in the signal sequence of the maltose-binding protein, *malE18-1*. The resulting double mutant OLF760 (MC4100 *zjb*::Tn*5 malE18-1 secY1004*) was completely defective in MalE export and had a Mal$^-$ phenotype on MacConkey maltose indicator media. This strain was transformed with the pOFY7, pOFY8, or pOFY9 plasmid, carrying the proximal, middle, or distal third, respectively, of the wild-type *secY* gene, constructed as described previously (16). In a marker rescue experiment, only the plasmid pOFY7 restored the Mal$^+$ phenotype on maltose minimal Amp plates, with a frequency of about 10^{-5}, corresponding to the rate of homologous recombination. The corresponding fragment from strain OFM1004 was PCR amplified and sequenced to identify a single mutation causing an E108K substitution in the second cytoplasmic loop of SecY.

The lesion in mutant OFM4004, conferring a weak cold-sensitive phenotype, was cotransduced by P1 with the *tsx*::*kan* marker and, therefore, is linked to the *secDF* locus. The Lac$^+$ phenotype of strain OFM4004 (pOF21) could be converted to Lac$^-$ when cotransformed with the compatible plasmid pCHAP8096 carrying wild-type *secD*, but not with pCHAP8092 carrying wild-type *secF*, suggesting that the Lac$^+$ phenotype was due to a *secD* mutation. This was confirmed by DNA sequence analysis of PCR-amplified *secD* from OFM4004, which indicated a G506D substitution in the fourth transmembrane segment of SecD.

The Lac$^+$ mutation in strain OFM1610 was cotransduced with the *argE* locus and, therefore, is linked to the *secE* gene. Plasmid pCHAP8095, carrying wild-type *secE*, restored the original Lac$^-$ phenotype. Sequence analysis of the PCR-amplified *secE* gene from this mutant revealed a single G to A nucleotide change at position −38 relative to the *secE* start codon. This mutation presumably reduces the level of *secE* expression. The mutation in strain OFM7004, identified in the same selection, was genetically linked to the *leu* marker at min 2 of the *E. coli* chromosome and mapped to the *secM-secA* operon. The mutation was designated *secA7004*, although it could be in the *secM* gene, and was not further characterized.

Protein analysis and enzymatic assays. Proteins were separated by sodium dodecyl sulfate-polyacrylamide gel electrophoresis (SDS-PAGE) on 10%, 12%, or 15% polyacrylamide gels with Tris-glycine and SDS buffers and then transferred electrophoretically to nitrocellulose membranes using a semidry blotting apparatus. Primary antibodies were rabbit antisera raised against purified MalE (J.-M. Betton), PulG, RbsB (17), GFP (Clontech), DsbA (Satish Raina), MalE-PulC, MalE-PulS, Pal (Emmanuelle Bouveret), DjlA (David Clarke), and LacZ (Organon Teknika Corp.). Secondary antibodies were donkey anti-rabbit immunoglobulin G coupled to horseradish peroxidase (Amersham Biosciences). Antibody-treated nitrocellulose membranes were developed by enhanced chemiluminescence (Amersham). β-Galactosidase activity was assayed according to Miller (32). Pullulanase cell surface exposure was assayed as described previously (31).

Pulse-chase and immunoprecipitation analyses. Cells were grown overnight in M63 medium containing 0.5% glycerol and diluted 1:100 in fresh M63 medium containing 0.5% glycerol or 0.2% glycerol and 0.4% maltose supplemented with a cocktail of 18 amino acids (lacking methionine and cysteine). Cells were grown to an optical density at 600 nm (OD_{600}) of 0.4 and pulse-labeled for 15 s with 10 μCi/ml of [^{35}S]methionine, followed by a 1-min chase in the presence of cold methionine (100 μg/ml) and chloramphenicol (170 μg/ml). Samples of 1 ml were withdrawn at the indicated times (see the legend to Fig. 1B) and precipitated with 5% trichloroacetic acid for 30 min on ice. After 10 min of centrifugation in a microcentrifuge at 4°C, pellets were washed twice with 1 ml of cold acetone and air dried. For immunoprecipitation, total extracts were resuspended in 50 μl of 25 mM Tris-HCl (pH 8) buffer containing 1% SDS and 1 mM EDTA and heated at 100°C for 2 min. After cooling to room temperature, 450 μl KI buffer (50 mM Tris-HCl [pH 8.0], 150 mM NaCl, 2% Triton X-100, 1 mM EDTA) was added and samples were centrifuged for 10 min in a microcentrifuge at 4°C. A 200-μl aliquot was taken from each tube and further diluted with 300 μl of ice-cold KI buffer. Anti-MalE antiserum (final dilution, 1:500) was added to each sample, and the samples were incubated overnight on ice. Protein A-coated Sepharose (Amersham Biosciences) was added to each tube and incubated for 20 min on ice with mixing. The samples were centrifuged for 1 min in a microcentrifuge, and supernatants were removed. Pellets were washed twice with 0.5 ml of 50 mM Tris-HCl (pH 8.0), 1 M NaCl, 1% Triton X-100 and once with 10 mM Tris-HCl (pH 8.0). The pellets were resuspended in 50 μl SDS-PAGE sample buffer and heated to 100°C for 2 min to release proteins bound to the beads. The samples were then analyzed by SDS-PAGE and fluorography.

***E. coli* fractionation and sucrose gradient separation.** Spheroplast and periplasmic fractions were prepared as described previously (44). Bacteria were grown to mid-log phase and total cell and spheroplast fractions were resuspended in SDS sample buffer at a concentration corresponding to 10 OD_{600} units/ml. Periplasmic fractions were precipitated in 10% trichloroacetic acid for 30 min on ice and then pelleted for 10 min in a microcentrifuge at 4°C. After two washes with 1 ml of cold acetone, pellets were air dried and resuspended in the appropriate volume of sample buffer based on the fraction of the total volume concentration relative to that of the spheroplast samples.

Sucrose gradient fractionation of membranes containing PulG or PulG-mRFP was performed as described previously (46). Fractions from the gradients were analyzed by SDS-PAGE on 10% or 12% acrylamide gels, followed by immunoblotting with antibodies against PulG, PulC, PulS, Pal, and DjlA.

Fluorescence microscopy and plasmolysis. For fluorescence microscopy, strains were grown overnight at 30°C, diluted 1 to 100 in fresh medium, and grown to an OD_{600} of 0.2. Isopropyl β-D-thiogalactoside (IPTG) was then added to a final concentration of 10 or 100 μM and 0.4% maltose was added for strains carrying the *pul* genes under MalT-dependent promoter control. The cells were incubated for 1 h at 30°C under continuous shaking. Live cells were immobilized on wet agarose-coated glass slides and analyzed using a Zeiss Axioplan 2 fluorescence microscope with a Hamamatsu CCD camera mounted. Images were collected using OpenLab software and processed with Photoshop. Cells were plasmolyzed as described elsewhere (27) prior to examination.

RESULTS

Construction and analysis of a PulG-LacZ hybrid. Protein fusions to β-galactosidase (LacZ) have been useful tools for the genetic analysis of many biological functions, in particular, protein localization and export. When proteins with signal peptides are fused to LacZ and targeted to extracytoplasmic compartments in *E. coli*, the LacZ domain becomes enzymatically inactive and the bacteria are phenotypically Lac$^-$. Mutations conferring a Lac$^+$ phenotype by causing localization of LacZ fused to periplasmic MalE to the cytoplasm contributed to the discovery of the first Sec pathway components, SecA (35) and SecB (26). A similar approach based on LacZ fused to the IM protein MalF led to the identification of a pathway involved in periplasmic disulfide bond formation (30). Other genetic (59) and biochemical (28, 60) approaches identified the signal recognition particle (SRP) as a key component for IM protein biogenesis in *E. coli*. Recently, a modification of the MalF-LacZ selection produced mutants affected in all known components of the SRP pathway (*ffh*, *ffs*, and *ftsY*) (58). Therefore, we reasoned that the LacZ fusion approach should be sufficiently sensitive to identify factors required for PulG localization.

TABLE 3. β-Galactosidase activities of different *E. coli* strains expressing the *pulG-lacZ* gene fusion

Strain	Genotype	β-Galactosidase activity [Miller units (±SD)][a]		Mutant/ wild type ratio[b]
		−Maltose	+Maltose	
MC4100	Wild type	0.2 (±0.1)	0.2 (±0.1)	1
PAP5237	*dsbA*::kan	14.5 (±5.5)	47.5 (±17.8)	39
PAP5250	*dsbB*::kan	23.9 (±8.9)	32.2 (±9.6)	150
MC4100 Δ*secB*	Δ*secB*	ND	0.3 (±0.1)	ND
MM52	*secA51*(Ts)	5.0 (±2.9)	12.9 (±4.3)	21
MC4100 *secY24*	*secY24*(Ts)	7.4 (±1.4)	16.7 (±7.2)	60
OFM1004	*secY108*	22.2 (±6.8)	46.5 (±3.1)	154
OFM7004	*secA7004*	1.1 (±0.8)	5.1 (±2.2)	3
OFM4004	*secD4004*	1.0 (±0.4)	4.9 (±3.3)	6
MC4100 *secE*(Cs)	*secE15*(Cs)	2.3 (±1.3)	16.5 (±11.8)	10
OFM1610	*secE1610*	3.6 (±2.0)	6.5 (±3.1)	16
AD208	*secY39*(Cs)	ND	30.8 (±2.4)	ND
TY22	*secY40*(Cs)	ND	27.7 (±4.8)	ND

[a] β-Galactosidase activity of cells grown in the absence (−) or presence (+) of 0.4% maltose in LB growth medium. The mean values from at least three independent experiments are given, with standard deviations indicated in parentheses.

[b] β-Galactosidase activities in mutants normalized against activity in the wild-type strain, all grown without maltose, with values obtained after subtracting the standard deviation from the mean. ND, not determined.

A full-length *pulG* gene lacking its stop codon was fused to *lacZ* lacking its 8 N-terminal codons on a moderate-copy-number plasmid, pCHAP8075 (described in Materials and Methods). The *pulG-lacZ* fusion was expressed from the p*malE* promoter and transcribed in an operon with the downstream *lacY* and *lacA* genes. *E. coli* MC4100 transformed with this plasmid produced pale blue colonies on X-Gal indicator plates and was Lac$^-$ on tetrazolium-lactose agar. The manifestly low level of β-galactosidase in this strain could be explained by the targeting of the chimera to the membrane. To ensure that the Lac$^-$ phenotype of strain MC4100(pCHAP8075) was due to a low specific activity and not to low-level synthesis of the chimera, pCHAP8075 was introduced into strains carrying mutations in the disulfide bond formation factor genes *dsbA* and *dsbB*. The specific β-galactosidase activity of the PulG-LacZ hybrid increased substantially in these strains (Table 3), indicating that disulfide bonds in periplasmically exposed LacZ stabilize the transmembrane conformation of the PulG-LacZ hybrid (55).

Immunoblot analysis of strain MC4100(pCHAP8075) confirmed the synthesis of a stable maltose-inducible hybrid protein that reacted with both anti-PulG and anti-LacZ antibodies (Fig. 1A). As described previously (22), the induction of MalE-LacZ synthesis in strain MM18 caused pleiotropic defects in protein export, including the accumulation of unprocessed, signal peptide-containing forms of MalE and ribose-binding protein (RbsB). In contrast, maltose-induced production of PulG-LacZ did not cause any export defects (Fig. 1A). Efficient MalE export under these conditions was confirmed by pulse-chase analysis (Fig. 1B). More than 95% of MalE was in the mature form after 15 s of pulse-labeling in both wild-type MC4100 and MC4100(pCHAP8075). Significant precursor accumulation was observed in strain MM52, which carries the *secA51*(Ts) mutation and was used as a control. These results indicate that the properties of the PulG-LacZ hybrid protein are different from those of MalE-LacZ, suggesting underlying differences in the ways the two chimeras are targeted for export. Indeed, as discussed below, the phenotype of cells producing PulG-LacZ is reminiscent of that of cells producing a LamB-LacZ variant with an abnormally hydrophobic signal peptide (65).

Influence of *sec* mutations on PulG-LacZ localization. To identify targeting factors involved in PulG membrane insertion, the PulG-LacZ hybrid was introduced into *E. coli* MC4100 derivatives with mutations affecting known protein export factors. Specific β-galactosidase activity was used as a measure of PulG-LacZ localization under conditions of basal and maltose-induced *pulG-lacZ* expression (Table 3). The Δ*secB* mutation was without effect, indicating that SecB is not involved in PulG membrane targeting. The *secA51*(Ts) mutation led to a 20-fold increase in β-galactosidase activity under semipermissive conditions, and *secY24*(Ts) had an even more pronounced effect. The greatest increase in β-galactosidase activity was observed in the *secY108* mutant. The novel *secY108* mutant, isolated in a screen for mutants defective in localization of LacZ fused to ribose-binding protein RbsB (Francetic and Kumamoto, unpublished results), has an E108K change in the second cytoplasmic loop of SecY. The *secD4004* and *secE1610* mutations identified in the same screen had a weaker effect on the export of PulG-LacZ.

The two cold-sensitive mutations *secY39* and *secY40*, shown previously to affect IM protein insertion (1, 34), both led to substantially impaired PulG-LacZ membrane localization at

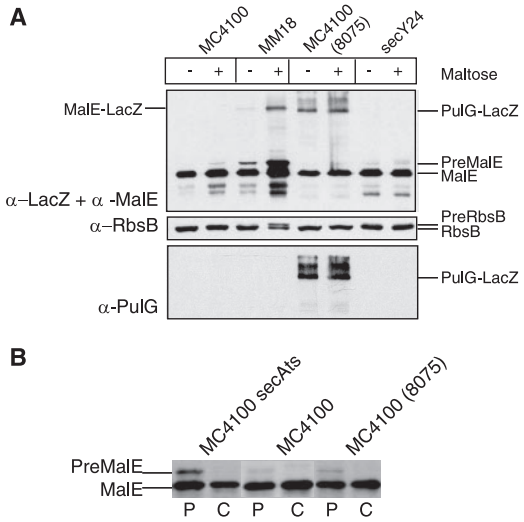

FIG. 1. Induction of the PulG-LacZ fusion synthesis has no effect on substrates of the Sec pathway. (A) Cells of strains MC4100, MM18, MC4100(pCHAP8075), and MC4100 *secY24*(Ts) were grown at 30°C in LB medium containing Amp in the absence (−) or presence (+) of 0.2% maltose for 3 h with vigorous shaking. Total cell extracts were analyzed by SDS-PAGE and immunoblotting using anti-LacZ, anti-MalE, anti-RbsB, and anti-PulG antisera, as indicated at the bottom left of each panel (α, anti). The positions of relevant proteins are indicated on the right. (B) Pulse-chase analysis of MalE export in strains MC4100, MM4100 *secA*(Ts) (MM52) (left 2 lanes), and MC4100 (pCHAP8075) (right 2 lanes). Cells were grown at 30°C in minimal maltose medium, pulse-labeled with [^{35}S]methionine for 15 s (P), and chased for 60 s (C). Labeled cell extracts were immunoprecipitated with anti-MalE antibodies. Proteins were analyzed by SDS-PAGE and fluorography. The relevant portion of the resulting fluorogram is shown. The positions of PreMalE and MalE proteins are indicated.

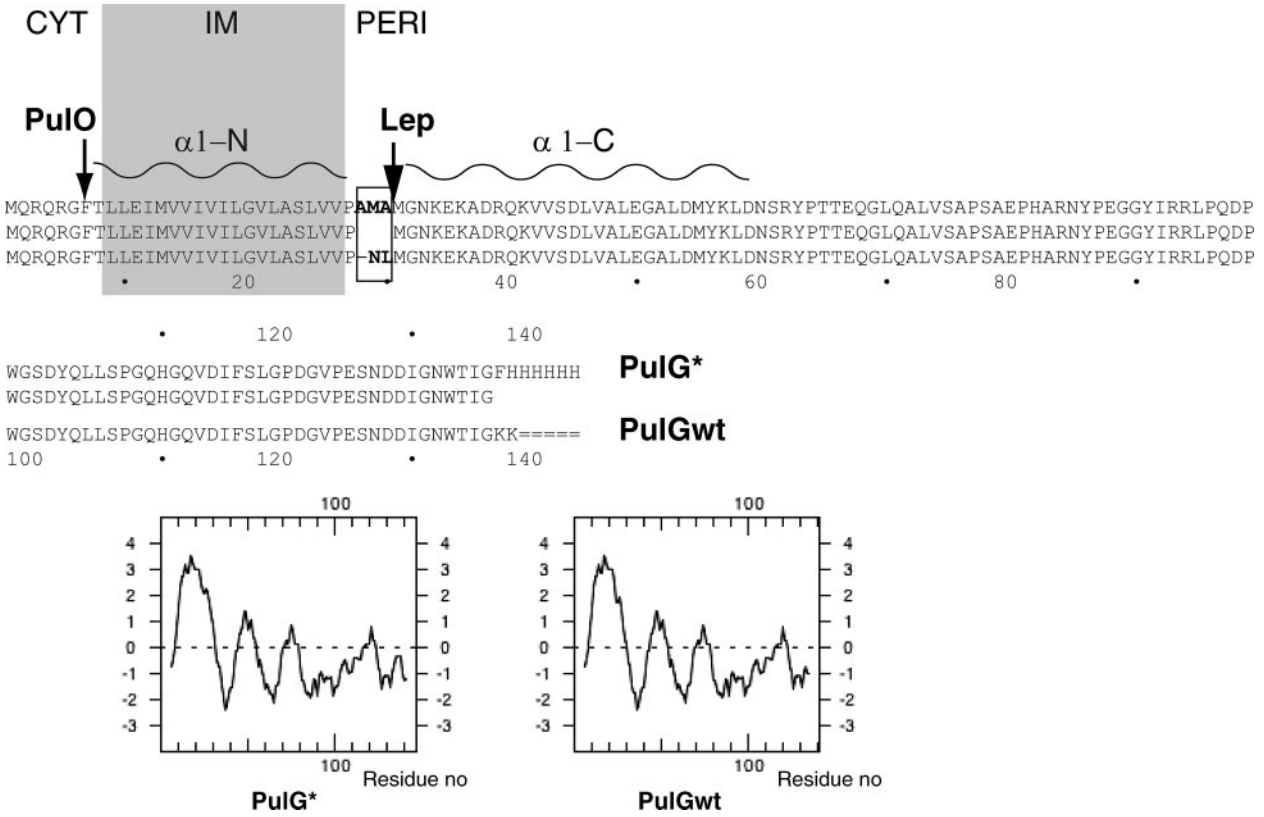

FIG. 2. Engineering the leader peptidase cleavage site in PulG. The primary sequence alignment of wild-type PulG and PulG* is shown, with sequence mismatches indicated with a rectangle. The position of the PulG sequence with respect to the cytoplasmic (CYT), inner membrane (IM), and periplasmic (PERI) compartments is shown. Arrows indicate the prepilin peptidase PulO and leader peptidase Lep cleavage sites. The wavy lines indicate the hydrophobic inner membrane (α-1N) and periplasmic amphipathic (α-1C) alpha helical domains. Kyte-Doolittle hydropathy plots of PulG* and wild-type PulG (PulGwt) are shown.

the semipermissive temperature. Since both of these mutations show a synthetic lethal phenotype when combined with deficiencies in the SRP pathway, their rather strong effect, in particular that of *secY40*, pointed to a possible SRP involvement in PulG targeting. A role for SRP was expected, based on the high level of hydrophobicity of the N-terminal α-helical domain of PulG (Fig. 2) (21).

PulG membrane insertion assay. Several approaches have been used in the biochemical analysis of IM protein insertion (20, 23, 29, 30). Although processing of PrePulG by PulO prepilin peptidase can be used as an indicator of export, only six amino acids are removed, making it difficult to resolve precursor and mature forms (40). Furthermore, PrePulG processing occurs on the cytoplasmic side of the IM and might occur without membrane insertion. To facilitate the analysis of PulG membrane insertion, we created PrePulG* by replacing two amino acids downstream from the transmembrane (TM) helix α-N1 of PulG (Fig. 2) with an artificial leader peptidase cleavage site (pCHAP8086; described in Materials and Methods). In MC4100 F′ *lacI*^{q1}(pCHAP8086), the majority of PulG* was found in its processed form, corresponding in size to the periplasmic domain of PulG (residues 25 to 140 of mature PulG), in the soluble, periplasmic fraction (Fig. 3A, wt). In contrast, significant accumulation of the unprocessed PrePulG* was observed in strains MC4100 *secY108* and MC4100 *secA7004* (Fig. 3A). The level of PrePulG* in these strains correlated well with the levels of export defects of the PulG-LacZ fusion observed in the same mutants (Table 3). Similarly, processing of PrePulG* was defective in MC4100 mutants *secE1610* and *secD4004* and in *secA51*(Ts) at 37°C (Fig. 3B and C). Processing of PreMalE was affected in all of the *sec* mutants.

The cold-sensitive mutation *secY40* (strain TY22) specifically affects the insertion of IM proteins (34), unlike the *secY39* allele (strain AD208) that affects the export of both IM and periplasmic (and outer membrane) proteins (1, 34). To determine the extent of the PrePulG* processing and release in the two strains, we introduced an F′ *lacI*^{q1} episome by mating with strain CK1637 F′ *lacI*^{q1}. However, the resulting strains showed a growth defect when transformed with plasmid pCHAP8086, and PulG* could not be detected in their extracts. Only when PrePulG* was encoded by the low-copy-number plasmid pCHAP8100 could PulG* insertion be analyzed by fractionation in these mutants. In agreement with the LacZ activity measurements (Table 3), weak accumulation of PrePulG* was observed in both mutant strains. Overlapping bands cross-reacting with the anti-PulG antibodies made it difficult to quantify this defect in PrePulG* processing. As expected, the export of MalE was specifically defective only in strain AD208

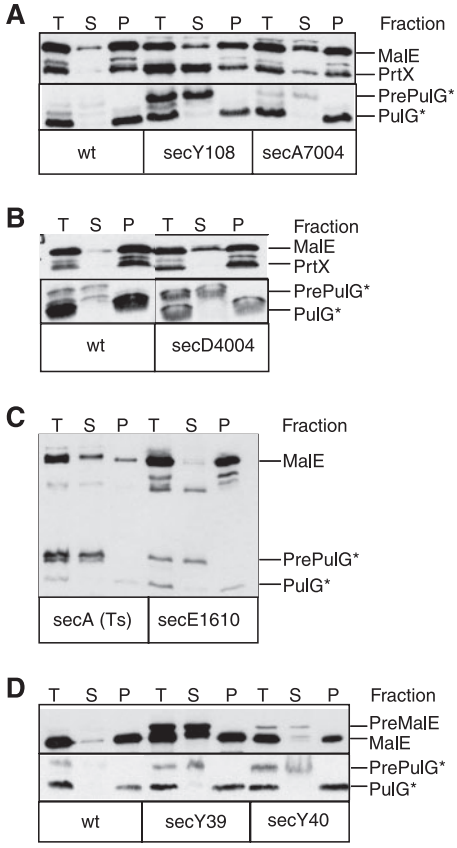

FIG. 3. Fractionation analysis of PulG* membrane insertion in wild-type MC4100 (wt) and *secA7004*, *secA51*(Ts) [secA (Ts)], *secY108*, *secD4004*(Cs), *secE1610*, *secY39*(Cs), and *secY40*(Cs) mutants. All strains are derived from MC4100 and carry the F′ *lacI*^{q1} episome pAPIP501 (Table 1). Bacteria were grown at 30 or 37°C in LB media supplemented with Amp or chloramphenicol to an OD_{600} of 0.8 and subjected to fractionation as described in Materials and Methods. Total cell (T), spheroplast (S), and periplasmic (P) fractions corresponding to 0.05 OD_{600} unit were analyzed with 12% SDS-PAGE and transferred onto nitrocellulose membranes. The membranes were probed with anti-PulG and anti-MalE antibodies. The positions of full-length PrePulG* and processed PulG* and MalE are indicated. A band reacting nonspecifically with the anti-MalE antiserum is labeled PrtX.

F′ *lacI*^{q1}, with only very-low-level PreMalE accumulation being observed in strain TY22 F′ *lacI*^{q1} (Fig. 3D).

Strain JS7131 carrying a p*araBAD-yidC* operon fusion and transformed with plasmid pCHAP8086 was used to test the effect of YidC on PrePulG*. No differences in PrePulG* processing were observed upon removal of arabinose (data not shown), which leads to YidC depletion (48). Immunoblotting revealed a substantial accumulation of PspA after arabinose removal, indicating that YidC levels were reduced (61).

Depletion of the SRP component Ffh completely abolished PrePulG* processing. To test the involvement of the SRP pathway in PulG export, we introduced plasmid pCHAP8086 into the *ffh* conditional mutant WAM121 (p*araBAD-ffh*) (13). When WAM121(pCHAP8086) was grown in LB with 0.2% arabinose, PrePulG* was processed by leader peptidase, albeit less efficiently than in wild-type strains (Fig. 4). However, in cells grown in the presence of glucose (i.e., not expressing *ffh*),

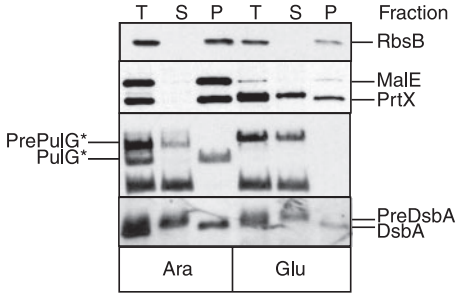

FIG. 4. Depletion of the SRP component Ffh prevents PrePulG* processing and membrane insertion. Cells of strain WAM121 (pCHAP8086) were grown overnight in LB medium supplemented with arabinose. The cells were washed twice with LB medium, diluted 1:50 into fresh LB medium supplemented with arabinose (Ara) or glucose (Glu), and grown to an OD_{600} of 0.8. Total extracts (T) and spheroplast (S) and periplasmic fractions (P) from 0.05 OD_{600} unit of bacteria were separated on 10% and 12% SDS-PAGE gels and transferred to nitrocellulose membranes, which were probed with antisera against PulG, MalE, RbsB, and DsbA. A band reacting nonspecifically with the anti-MalE antiserum is labeled PrtX.

PrePulG* processing was completely abolished, while the processing of MalE and RbsB was unaltered, indicating that the Sec machinery was still functional. Interestingly, the cross-reacting band, migrating at about 29 kDa, detected by anti-MalE antibodies (labeled PrtX in Fig. 4), was also sensitive to SRP depletion. The processing and periplasmic release of DsbA, a known SRP pathway substrate (52), were more defective in WAM121 in the presence of glucose, and the protein was less abundant.

PulG localization analyzed by fluorescence microscopy. PulG is a relatively abundant component of the Pul secreton and is assembled into periplasmic filaments during pullulanase secretion. The hydrophobic region of PulG is required for SRP-dependent export (this study) as well as for filament assembly and for retention in the membrane in the unassembled state (24, 39). Previous attempts using sucrose gradient fractionation to determine the site where unassembled PulG accumulates gave ambiguous results (37, 42), and the authors of a study with the PulG homolog XcpT proposed that its localization might change upon processing and activation of the secreton (5). We previously described the cellular localization of two other components of the Pul secreton analyzed by fluorescence microscopy of GFP chimeras (10). Here, we used a similar approach to study the localization of PulG in live *E. coli* cells.

In the absence of Pul secreton factors, GFP-PrePulG was localized at the periphery of MC4100 cells expressing chromosomal *gfp-pulG* in strain PAP9102 and induced with 100 μM IPTG. Occasional brighter patches were observed, similar to GFP-PulM hybrid proteins seen previously (10). In the presence of the Pul secreton factors encoded by pCHAP710, the hybrid protein was cleaved at the prepilin peptidase recognition site on the cytoplasmic face of the IM, releasing the GFP moiety with a short peptide derived from the N terminus of PrePulG (labeled GFP*) to the cytoplasm (Fig. 5A and B, lanes 4 to 6). Low-level proteolysis observed in the absence of the Pul factors (Fig. 5B, lanes 1 to 3) could be due to one or both of the chromosomally encoded *E. coli* prepilin peptidases

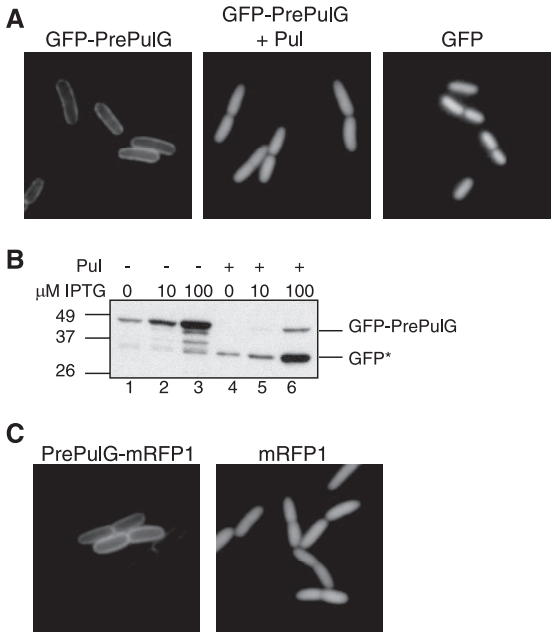

FIG. 5. Processing and localization of GFP-PrePulG in vivo. (A) Localization of GFP-PrePulG in wild-type *E. coli* strain MC4100. The left panel shows the expression of *pulG-gfp* from the chromosomal copy in strain PAP9102 induced with 100 μM IPTG. The center panel shows the processing of GFP-PrePulG in strain PAP9102 carrying plasmid pCHAP710, which encodes the complete Pul secretion system. The right panel shows the localization of the cytoplasmic GFP produced in strain PAP9121. (B) Production of GFP-PrePulG hybrid proteins in strains PAP9102 and PAP9102(pCHAP710) analyzed by immunoblot using anti-GFP antibodies (Clontech). The levels of the GFP-PrePulG hybrid protein induced by increasing concentrations of IPTG in the absence (−, lanes 1, 2 and 3) or presence (+, lanes 4, 5 and 6) of Pul secreton factors are indicated. The migration and mass (kDa) of the molecular size markers are indicated on the left. (C) Membrane localization of PrePulG-mRFP1 in the wild-type *E. coli* strain MC4100 carrying pCHAP7516 (left, PrePulG-mRFP1) or pCHAP7520 (right, cytoplasmic mRFP1).

(18). Fluorescence microscopy of plasmolyzed cells producing GFP-PrePulG indicated that the protein was almost entirely located in the inner membrane (Fig. 6A), as shown previously for GFP-PulM (27).

Fusing PulG to mRFP1 (11), which can fold correctly in the *E. coli* periplasm (27), allowed the effect of other Pul factors on the localization of PulG to be analyzed. The localization pattern of this chimera, encoded by plasmid pCHAP7520, was essentially the same as that of GFP-PrePulG (Fig. 5C and 6B). The maltose-induced production of Pul secreton factors did not change the distribution of PulG-mRFP1 inside cells, which remained IM associated (Fig. 6C). These data resolve previously ambiguous fractionation PulG data. For example, PulG fractionated mainly with the IM during sucrose gradient centrifugation but substantial amounts were also found in the outer membrane (OM) compared to the amounts of other IM proteins such as PulC and DjlA (Fig. 7A). The distribution of PulG-mRFP, as determined by fractionation, was similar to that of PulG, irrespective of whether the Pul secreton factors were present (Fig. 7B). Thus, the prepilin signal sequence of PulG probably anchors it mainly in the IM but substantial amounts (as much as 50% in some experiments, e.g., Fig. 7B, lower panel) might reassociate with the OM when the cells are disrupted.

DISCUSSION

Properties of the prepilin signal sequence explain the mechanism of PulG export. On the basis of studies with LacZ chimeras and with derivatives with an artificial leader peptidase cleavage site downstream from the prepilin signal sequence, we conclude that the SRP and Sec pathways are directly involved in the export of the pseudopilin PulG and, by inference, of all pseudopilins and related type IV pilins. PrePulG presumably inserts into the IM according to the positive-inside rule (62), with the positively charged N-terminal region of its prepilin signal sequence and prepilin peptidase cleavage site facing the cytoplasm and the C-terminal globular domain in the periplasm. This orientation is consistent with the fact that fusion of alkaline phosphatase (45) and β-lactamase (39) to the C terminus of full-length or truncated PulG leads to enzymatically active, periplasmically oriented membrane proteins and with the presence in pseudopilin PulK (41) and type IV pilins (12) of an intramolecular disulfide bond whose formation is catalyzed by periplasmic DsbA.

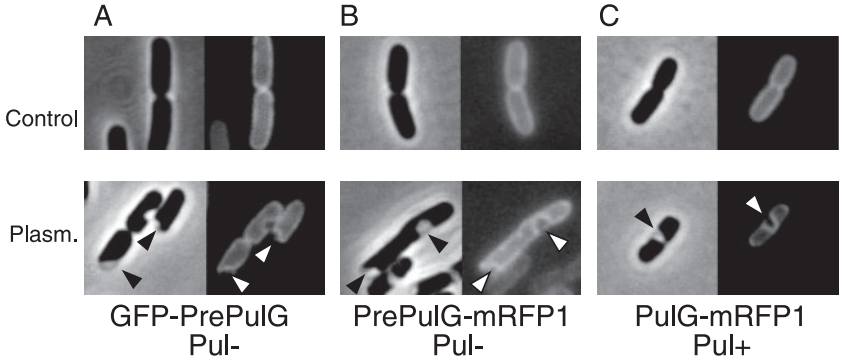

FIG. 6. Inner membrane localization of PulG. GFP-PrePulG was produced from the chromosome in strain PAP9102 under 10 μM IPTG induction (A) or as a C-terminal mRFP fusion from plasmid pCHAP7516 in strain PAP7500BG without (Pul^-) (B) or with (Pul^+) (C) the presence of 0.2% maltose to induce production of Pul secretion factors. By using fluorescence microscopy, hybrid proteins were located in the envelope of untreated cells (Control) or specifically in the IM from the OM (Plasm.). The arrowheads indicate plasmolysis bays. Each panel consists of a phase-contrast image (left) and the corresponding fluorescence image (right).

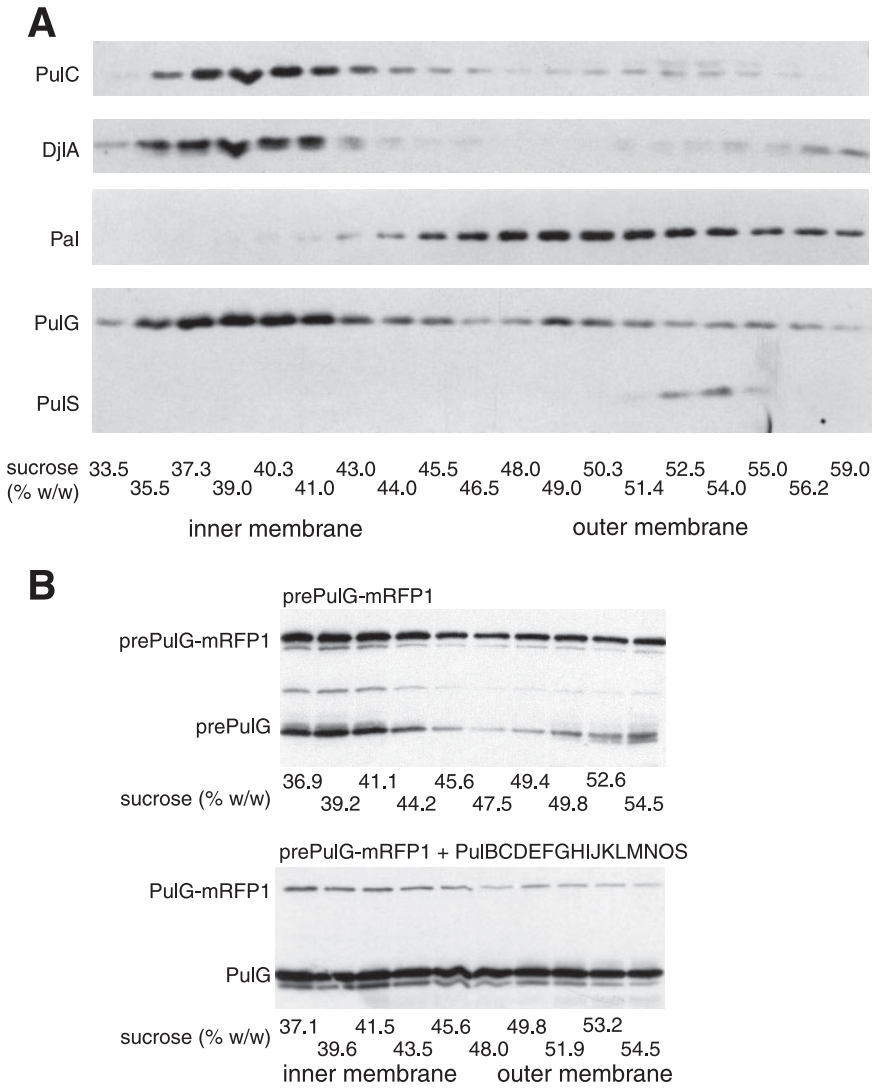

FIG. 7. Flotation sucrose gradient fractionation of PulG (A) and PulG-mRFP (B). Membranes obtained by French press disruption of cells of *E. coli*(pCHAP231) (A) or *E. coli*(pCHAP7516) with (B, lower panel) or without (B, upper panel) pCHAP710 (encoding all Pul secreton factors) were harvested from the gradients and analyzed by immunoblotting with antibodies against PulC, DjlA, Pal, PulS, (A), and PulG (A and B). The positions of the inner and outer membranes are indicated. Note that PrePulG-mRFP is partially degraded to a form similar in size to PrePulG (B, upper panel) and that this band is probably the faster migrating of the two bands recognized by the antibodies when the bacteria also produced PulG encoded by pCHAP710 (B, lower panel).

The prepilin signal sequence promotes export though the Sec translocon, anchors the protein in the inner membrane, and promotes subunit assembly into a pseudopilus or type IV pilus filament. The first two functions are independent of the sequence of the prepilin signal sequence, but pilus assembly requires precise interactions between residues in the signal sequences of adjacent protomers that are highly conserved in all members of the pseudopilin/type IV pilin family. The very high hydrophobicity of the prepilin signal sequence (Fig. 2) (13, 21, 60) presumably explains the absolute requirement for SRP for targeting to the Sec translocon. The data presented here rule out the possibility that secreton components, and in particular the PulCEFLM complex (38), are involved in pseudopilin translocation across the IM. Instead, this complex extracts the prepilin signal sequence from the IM and permits its interaction with adjacent prepilin signal sequences in the assembling filament. Arts et al. (3) report essentially identical conclusions in the accompanying paper on the export of the PulG homolog XcpT from *Pseudomonas aeruginosa*. In the following paragraphs, we discuss specific features of the SRP and Sec requirements for PulG.

SRP. The role of the SRP pathway in cotranslational IM protein biogenesis is now clearly established. The alternative, YidC-only pathway is used by a small number of proteins (48, 61). Here we present strong evidence for the involvement of SRP but not YidC in PulG targeting. The PulG-LacZ hybrid protein failed to jam the export machinery when overproduced. This is in marked contrast to other LacZ chimeras, such as MalE-LacZ and LamB-LacZ, which are toxic because they jam the Sec export machinery. However, a LamB-LacZ chi-

mera in which the hydrophobicity of the LamB signal peptide had been artificially increased was not toxic because it was routed to the Sec machinery via SRP and was translocated cotranslationally (65). Thus, PulG-LacZ is very similar to this LamB-LacZ variant. Depletion of the SRP component Ffh had the most dramatic effect of any of the conditions tested on PulG export, and the lack of posttranslational processing of PulG with an artificial leader peptidase cleavage site is also consistent with cotranslational PulG membrane insertion.

The Sec translocon. In vivo studies showed that SRP targets IM proteins to the SecYEGDF translocon for insertion (23, 60), while in vitro cross-linking of nascent IM proteins revealed contacts with Ffh, Fts, SecY, and SecA (43, 52). SecA is required for the insertion of IM proteins with periplasmic loops longer than 30 amino acids (1, 19, 43), while single-spanning IM proteins such as PulG always require SecA, regardless of the length of their periplasmic domain (15). Consistent with this, SecA depletion almost completely abolished PrePulG* processing. Several integral Sec membrane components were also shown to be required, including SecD, which is affected by the novel *secD4004* mutation that introduces a charged residue (G506D) in the fourth transmembrane segment, in a region highly conserved in members of the SecD family.

The *secY108*A mutation exerted a particularly strong effect on PulG insertion. The charge inversion in the second cytoplasmic loop of the SecY E108K variant could affect the interaction with SecA. The cold-sensitive alleles *secY39* and *secY40* also diminished PulG-LacZ export, consistent with their synthetically lethal effect when combined with defects in the SRP pathway (34). The residues affected by *secY39* (R357H) and *secY40* (A363T) both map in the fifth cytoplasmic loop of SecY and affect a translocation step subsequent to substrate binding (33). The mutation *secY40* appears to interfere with docking of the SRP receptor FtsY to the translocon (2). Export of the aforementioned LamB-LacZ hybrid that was redirected to the SRP pathway (65) was specifically affected only by the *secY40* allele, but this was not the case with PulG or with DsbA, another SRP substrate (54). Interestingly, overproduced PulG was specifically degraded in both of these *secY* mutants, possibly by cytoplasmic proteases Lon and ClpQ (8), whereas the accumulation of MalE was unaffected (data not shown).

Adding a leader peptidase cleavage site to PrePulG (to create PrePulG*) did not change the hydrophobicity of the prepilin signal sequence (Fig. 2), which presumably plays a decisive role in the choice of the targeting pathway. Processing of PrePulG* on the periplasmic side of the hydrophobic TM segment provided a direct kinetic assay for correct membrane insertion. However, pulse-chase analyses showed that PrePulG* is not processed posttranslationally, as observed for the DsbA protein, an SRP substrate with a natural cleavable signal sequence (52, 54). Therefore, we measured the steady-state levels of PulG by fractionation and immunoblotting as sensitive means to probe PulG insertion, especially in rich media that lead to more pronounced protein translocation defects (34). This approach also allowed detection of the weak MalE export defect in the *secY40* mutant that was not detected previously by pulse-chase analysis (4, 34). A defect in prepilin peptidase PulO-mediated processing of PulG was also demonstrated in SRP-depleted strains by using a variant of prePulG in which the propeptide was artificially extended with an N-terminal FLAG tag (data not shown). In the accompanying paper, Arts et al. show that processing of native XcpT, a close homologue of PulG, by prepilin peptidase also depends on SRP and the Sec machinery (3).

Localization of intracellular PulG pools. Previous studies with the *Vibrio cholerae* PulG homolog EpsG indicated that it clusters at the cell pole, consistent with the facts that type II secretion occurs at the pole in this bacterium and that other secreton components also accumulate there (53). In contrast, GFP-PrePulG and PulG-mRFP were evenly distributed throughout the *E. coli* inner membrane, consistent with previous data showing similar patterns of GFP-PulM and GFP-PulL distribution (10). The absence of clustering was surprising, since unassembled PulG can be chemically cross-linked into large complexes (39) that suggested the existence of discrete pools of PulG at distinct, putative assembly sites. However, neither PreGFP-PulG nor PulG-mRFP could be cross-linked into similar complexes, possibly because the fluorescent reporter interfered with clustering or with the positioning of amine groups in adjacent chimeras. The GFP-PrePulG chimera was functional, however, when cleaved by prepilin peptidase PulO. Thus, these data do not support the idea that PulG accumulates at specific assembly sites in the *E. coli* cell envelope, although we cannot exclude the possibility that native PulG might show a different distribution from that of fluorescent reporter-tagged PulG.

The analysis of PulG-mRFP1 indicates accumulation of unassembled PulG mainly or exclusively in the inner membrane. These data are inconsistent with sedimentation sucrose gradient fractionation of membranes derived by disrupting spheroplasts, which indicated OM association of PulG irrespective of the presence of other secreton components (42). Mainly inner membrane association of PulG was indicated here, however, by flotation sucrose gradient fractionation of membranes obtained by disrupting cells in a French pressure cell (Fig. 7A), although large amounts were again found in OM fractions, compared to the amounts of authentic inner membrane proteins. These studies underscore the intrinsic value of in situ localization using fluorescent reporter proteins (27) (Fig. 6), which are less subject to artifacts introduced during cell disruption and fractionation, although the reporter protein might not be entirely neutral. Importantly, none of the data in Fig. 6 and 7 indicate relocalization of PulG upon the expression of other Pul secreton factors. This makes it unlikely that the secreton relocalizes the major pseudopilin to the OM, as was proposed previously (5).

ACKNOWLEDGMENTS

We thank Harris Bernstein, Koreaki Ito, and Tom Silhavy for gifts of strains and for very helpful discussions; Jim Bardwell, Philippe Delepelaire, Ross Dalbey, and Jon Beckwith for strains; Roger Tsien for DNA encoding mRFP1; Jean-Michel Betton, Emmanuelle Bouveret, David Clarke, and Satish Raina for antibodies; Jan Tommassen for communicating data prior to publication; Benoit Arcangioli for the use of his microscope; Nathalie Nadeau for superb technical assistance; Sandy Niellez for help with plasmid construction; and members of the Pugsley lab and past members of the Kumamoto lab for their support and interest.

This work was supported in part by the Ministère Délégué à la Recherche et aux Nouvelles Technologies Programme de Microbiologie (grant ACIM 1-7) and by a postdoctoral fellowship from the Fondation pour la Recherche Medicale to N.B.

REFERENCES

1. **Andersson, H., and G. von Heijne.** 1993. *sec* dependent and *sec* independent assembly of *E. coli* inner membrane proteins: the topological rules depend on chain length. EMBO J. **12:**683–691.
2. **Angelini, S., S. Deitermann, and H. G. Koch.** 2005. FtsY, the bacterial signal-recognition particle receptor, interacts functionally and physically with the SecYEG translocon. EMBO Rep. **6:**476–481.
3. **Arts, J., R. van Boxtel, A. Filloux, J. Tommassen, and M. Koster.** 2007. Export of the pseudopilin XcpT of the *Pseudomonas aeruginosa* type II secretion system via the signal recognition particle-Sec pathway. J. Bacteriol. **189:**2063–2068.
4. **Baba, T., A. Jacq, E. Brickman, J. Beckwith, T. Taura, C. Ueguchi, Y. Akiyama, and K. Ito.** 1990. Characterization of cold-sensitive SecY mutants of *Escherichia coli*. J. Bacteriol. **172:**7005–7010.
5. **Bally, M., A. Filloux, M. Akrim, G. Ball, A. Lazdunski, and J. Tommassen.** 1992. Protein secretion in *Pseudomonas aeruginosa*: characterization of seven *xcp* genes and processing of secretory apparatus components by prepilin peptidase. Mol. Microbiol. **6:**1121–1131.
6. **Bardwell, J. C. A., K. McGovern, and J. Beckwith.** 1991. Identification of a protein required for disulfide bond formation in vivo. Cell **65:**581–589.
7. **Bartolomé, B., Y. Jubete, E. Martinez, and F. de la Cruz.** 1991. Construction and properties of a family of pACYC184-derived cloning vectors compatible with pBR322 and its derivatives. Gene **102:**75–78.
8. **Bernstein, H. D., and J. B. Hyndman.** 2000. Physiological basis for conservation of the signal recognition particle targeting pathway in *Escherichia coli*. J. Bacteriol. **183:**2187–2197.
9. **Boyd, D., D. S. Weiss, J. C. Chen, and J. Beckwith.** 2000. Towards single-copy gene expression systems making gene cloning physiologically relevant: lambda InCh, a simple *Escherichia coli* plasmid-chromosome shuttle system. J. Bacteriol. **182:**842–847.
10. **Buddelmeijer, N., O. Francetic, and A. P. Pugsley.** 2006. Green fluorescent chimeras indicate nonpolar localization of pullulanase secreton components PulL and PulM. J. Bacteriol. **188:**2928–2935.
11. **Campbell, R. E., O. Tour, A. E. Palmer, P. A. Steinbach, G. S. Baird, D. A. Zacharias, and R. Y. Tsien.** 2002. A monomeric red fluorescent protein. Proc. Natl. Acad. Sci. USA **99:**7877–7882.
12. **Craig, L., M. E. Pique, and J. A. Tainer.** 2004. Type IV pilus structure and bacterial pathogenicity. Nature Rev. **2:**363–378.
13. **de Gier, J.-W., P. Mansournia, Q. A. Valent, G. J. Phillips, J. Luirink, and G. von Heijne.** 1996. Assembly of a cytoplasmic membrane protein in *Escherichia coli* is dependent on the signal recognition particle. FEBS Lett. **399:**307–309.
14. **d'Enfert, C., A. Ryter, and A. P. Pugsley.** 1987. Cloning and expression in *Escherichia coli* of the *Klebsiella pneumoniae* genes for production, surface localization and secretion of the lipoprotein pullulanase. EMBO J. **6:**3531–3538.
15. **Dietermann, S., G. S. Sprie, and H.-G. Koch.** 2005. A dual function for SecA in the assembly of single-spanning membrane proteins in *Escherichia coli*. J. Biol. Chem. **280:**39077–39085.
16. **Francetic, O., M. P. Hanson, and C. A. Kumamoto.** 1993. *prlA* suppression of defective export of maltose-binding protein in *secB* mutants of *Escherichia coli*. J. Bacteriol. **175:**4036–4044.
17. **Francetic, O., and C. A. Kumamoto.** 1996. *Escherichia coli* SecB stimulates export without maintaining export competence of ribose-binding protein signal sequence mutants. J. Bacteriol. **178:**5954–5959.
18. **Francetic, O., S. Lory, and A. P. Pugsley.** 1998. A second prepilin peptidase gene in *Escherichia coli* K-12. Mol. Microbiol. **27:**763–775.
19. **Froderberg, L., E. Houben, J. C. Samuelson, M. Chen, S. K. Park, G. J. Phillips, R. Dalbey, J. Luirink, and J. W. De Gier.** 2003. Versatility of inner membrane protein biogenesis in *Escherichia coli*. Mol. Microbiol. **47:**1015–1027.
20. **Froshauer, S., and J. Beckwith.** 1984. The nucleotide sequence of the gene for MalF protein, an inner membrane component of the maltose transport system of *Escherichia coli*. Repeated sequences are found in the *malE-malF* intercistronic region. J. Biol. Chem. **259:**10896–10903.
21. **Huber, D., D. Boyd, Y. Xia, M. H. Olma, M. Gerstein, and J. Beckwith.** 2005. Use of thioredoxin as a reporter to identify a subset of *Escherichia coli* signal sequences that promote signal recognition particle-dependent translocation. J. Bacteriol. **187:**2983–2991.
22. **Ito, K., P. J. Bassford, and J. Beckwith.** 1981. Protein localization in *E. coli*: is there a common step in the secretion of periplasmic and outer membrane proteins? Cell **24:**707–717.
23. **Jander, G., J. E. J. Cronan, and J. Beckwith.** 1996. Biotinylation in vivo as a sensitive indicator of protein secretion and membrane protein insertion. J. Bacteriol. **178:**3049–3058.
24. **Köhler, R., K. Schäfer, S. Müller, G. Vignon, K. Driedrichs, A. Philippsen, P. Ringler, A. P. Pugsley, A. Engel, and W. Welte.** 2004. Structure and assembly of pseudopilin PulG. Mol. Microbiol. **54:**647–664.
25. **Kornacker, M. G., and A. P. Pugsley.** 1989. Molecular characterization of *pulA* and its product, pullulanase, a secreted enzyme of *Klebsiella pneumoniae* UNF5023. Mol. Microbiol. **4:**73–85.
26. **Kumamoto, C. A., and J. Beckwith.** 1983. Mutations in a new gene, *secB*, cause defective protein localization in *Escherichia coli*. J. Bacteriol. **154:**253–260.
27. **Lewenza, S., D. Vidal-Ingigliardi, and A. P. Pugsley.** 2006. Direct visualization of red fluorescent lipoproteins indicates conservation of the membrane sorting rules in the family *Enterobacteriaceae*. J. Bacteriol. **188:**3516–3524.
28. **MacFarlane, J., and M. Müller.** 1995. Functional integration of a polytopic membrane protein of *E. coli* requires the bacterial signal recognition particle. Eur. J. Biochem. **223:**766–771.
29. **McGovern, K., and J. Beckwith.** 1991. Membrane insertion of the *Escherichia coli* MalF protein in cells with impaired secretion machinery. J. Biol. Chem. **266:**20870–20876.
30. **McGovern, K., M. Ehrmann, and J. Beckwith.** 1991. Decoding signals for membrane protein assembly using alkaline phosphatase fusions. EMBO J. **10:**2773–2782.
31. **Michaelis, S., C. Chapon, C. d'Enfert, A. P. Pugsley, and M. Schwartz.** 1985. Characterization and expression of the structural gene for pullulanase, a maltose-inducible secreted protein of *Klebsiella pneumoniae*. J. Bacteriol. **164:**633–638.
32. **Miller, J. H.** 1972. Experiments in molecular genetics. Cold Spring Harbor Laboratory, Cold Spring Harbor, NY.
33. **Mori, H., and K. Ito.** 2001. An essential amino acid residue in the protein translocation channel revealed by targeted random mutagenesis of SecY. Proc. Natl. Acad. Sci. USA **98:**5128–5133.
34. **Newitt, J. A., and H. D. Bernstein.** 1998. A mutation in the *Escherichia coli secY* gene that produces distinct effects on inner membrane protein insertion and protein export. J. Biol. Chem. **273:**12451–12456.
35. **Oliver, D., and J. Beckwith.** 1981. *E. coli* mutants pleiotropically defective in the export of secreted proteins. Cell **25:**2765–2772.
36. **Possot, O., C. d'Enfert, I. Reyss, and A. P. Pugsley.** 1992. Pullulanase secretion in *Escherichia coli* K12 requires a cytoplasmic protein and a putative polytopic cytoplasmic membrane protein. Mol. Microbiol. **6:**95–105.
37. **Possot, O., and A. P. Pugsley.** 1994. Molecular characterization of PulE, a protein required for pullulanase secretion. Mol. Microbiol. **12:**287–299.
38. **Possot, O., G. Vignon, N. Bomchil, F. Ebel, and A. P. Pugsley.** 2000. Multiple interactions between pullulanase secreton components involved in stabilization and cytoplasmic membrane association of PulE. J. Bacteriol. **182:**2142–2152.
39. **Pugsley, A. P.** 1996. Multimers of the precursor of a type IV pilin-like component of the general secretory pathway are unrelated to pili. Mol. Microbiol. **20:**1235–1245.
40. **Pugsley, A. P.** 1993. Processing and methylation of PulG, a pilin-like component of the general secretory pathway of *Klebsiella oxytoca*. Mol. Microbiol. **9:**295–308.
41. **Pugsley, A. P., N. Bayan, and N. Sauvonnet.** 2001. Disulfide bond formation in secreton component PulK provides a possible explanation for the role of DsbA in pullulanase secretion. J. Bacteriol. **183:**1312–1319.
42. **Pugsley, A. P., and O. Possot.** 1993. The general secretory pathway of *Klebsiella oxytoca*: no evidence for relocalization or assembly of pilin-like PulG protein into a multiprotein complex. Mol. Microbiol. **10:**665–674.
43. **Qi, H.-Y., and H. D. Bernstein.** 1999. SecA is required for the insertion of inner membrane proteins targeted by the *Escherichia coli* signal recognition particle. J. Biol. Chem. **274:**8993–8997.
44. **Randall, L. L., and S. J. S. Hardy.** 1986. Correlation of competence for export with lack of tertiary structure of the mature species: a study *in vivo* of maltose-binding protein in *E. coli*. Cell **46:**921–928.
45. **Reyss, I., and A. P. Pugsley.** 1990. Five additional genes in the *pulC-O* operon of the gram-negative bacterium *Klebsiella oxytoca* UNF5023 that are required for pullulanase secretion. Mol. Gen. Genet. **222:**176–184.
46. **Robichon, C., M. Bonhivers, and A. P. Pugsley.** 2003. An intramolecular disulfide bond reduces the efficacy of a lipoprotein plasma membrane sorting signal. Mol. Microbiol. **49:**1145–1154.
47. **Sambrook, J., E. F. Fritsch, and T. Maniatis.** 1989. Molecular cloning: a laboratory manual, 2nd ed. Cold Spring Harbor Laboratory, Cold Spring Harbor, NY.
48. **Samuelson, J. C., M. Chen, F. Jiang, I. Möller, M. Wiedmann, A. Kuhn, G. J. Phillips, and R. E. Dalbey.** 2000. YidC mediates membrane protein insertion in bacteria. Nature **406:**637–641.
49. **Sandkvist, M.** 2001. Biology of type II secretion. Mol. Microbiol. **40:**271–283.
50. **Sauvonnet, N., G. Vignon, A. P. Pugsley, and P. Gounon.** 2000. Pilus formation and protein secretion by the same machinery in *Escherichia coli*. EMBO J. **19:**2221–2228.
51. **Schatz, P. J., K. L. Bieker, K. M. Ottemann, T. J. Silhavy, and J. Beckwith.** 1991. One of three transmembrane stretches is sufficient for the functioning of the SecE protein, a membrane component of the *E. coli* secretion machinery. EMBO J. **10:**1749–1757.
52. **Schierle, C. F., M. Berkmen, D. Huber, C. Kumamoto, D. Boyd, and J. Beckwith.** 2003. The DsbA signal sequence directs efficient, cotranslational export of passenger proteins to the *Escherichia coli* periplasm via the signal recognition particle pathway. J. Bacteriol. **185:**5706–5713.
53. **Scott, M., Z. Dossani, and M. Sandkvist.** 2001. Directed polar secretion of

protease from single cells of *Vibrio cholerae* via the type II secretion pathway. Proc. Natl. Acad. Sci. USA **94:**13978–13983.

54. **Shimohata, N., Y. Akiyama, and K. Ito.** 2005. Peculiar properties of DsbA in its export across the *Escherchia coli* cytoplasmic membrane. J. Bacteriol. **187:**3997–4004.
55. **Snyder, W. B., and T. J. Silhavy.** 1995. β-galactosidase is inactivated by intermolecular disulfide bonds and is toxic when secreted to the periplasm of *Escherichia coli*. J. Bacteriol. **177:**953–963.
56. **Takeshita, S., M. Sato, M. Toba, W. Masahashi, and T. Hashimoto-Goto.** 1987. High copy number and low copy number plasmid vectors for *lacZ* α-complementation and chloramphenicol- or kanamycin-resistance selection. Gene **61:**63–74.
57. **Taura, T., Y. Akiyama, and K. Ito.** 1994. Genetic analysis of SecY; additional export-defective mutations and factors affecting their phenotypes. Mol. Gen. Genet. **243:**261–269.
58. **Tian, H., D. Boyd, and J. Beckwith.** 2000. A mutant hunt for defects in membrane protein assembly yields mutations affecting the bacterial signal recognition particle and Sec machinery. Proc. Natl. Acad. Sci. USA **97:**4730–4735.
59. **Ulbrandt, N. D., J. A. Newitt, and H. D. Bernstein.** 1997. The *E. coli* signal recognition particle is required for the insertion of a subset of inner membrane proteins. Cell **88:**187–196.
60. **Valent, Q. A., D. A. Kendall, S. High, R. Kusters, B. Oudega, and J. Luirink.** 1995. Early events in preprotein recognition in *E.coli*: interaction of SRP and trigger factor with nascent polypeptides. EMBO J. **14:**5494–5505.
61. **van der Laan, M., M. L. Urbanus, C. M. ten Hagen-Jongman, N. Nouwen, B. Oudega, N. Harms, A. J. Driessen, and J. Luirink.** 2003. A conserved function of YidC in the biogenesis of respiratory chain complexes. Proc. Natl. Acad. Sci. USA **100:**5801–5806.
62. **von Heijne, G., and I. Gavel.** 1988. Topogenic signals in integral membrane proteins. Eur. J. Biochem. **174:**671–678.
63. **Weiss, D. S., J. C. Chen, J. M. Ghigo, D. Boyd, and J. Beckwith.** 1999. Localization of FtsI (PBP3) to the septal ring requires its membrane anchor, the Z ring, FtsA, FtsQ, and FtsL. J. Bacteriol. **181:**508–520.
64. **Whitchurch, C. B., M. Hobbs, S. P. Livingstone, V. Krishnapillai, and J. S. Mattick.** 1991. Characterization of a *Pseudomonas aeruginosa* twitching motility gene and evidence for a specialized protein export system widespread in bacteria. Gene **101:**33–44.
65. **Wilson-Bowers, C., F. Lau, and T. J. Silhavy.** 2003. Secretion of LamB-LacZ by the signal recognition particle pathway of *Escherichia coli*. J. Bacteriol. **185:**5697–5705.